Effect of phonon confinement on the thermoelectric figure of merit of quantum wells

Alexander Balandin[a] and Kang L. Wang
Electrical Engineering Department, Device Research Laboratory, University of California–Los Angeles, Los Angeles, California 90095-1594

(Received 24 July 1998; accepted for publication 25 August 1998)

Recently, it has been shown that the thermoelectric figure of merit is strongly enhanced in quantum wells and superlattices due to two-dimensional carrier confinement. We predict that the figure of merit can increase even further in quantum well structures with free-surface or rigid boundaries. This additional increase is due to spatial confinement of acoustic phonons and corresponding modification of their group velocities. The latter leads to an increase of the phonon relaxation rates and thus, a significant drop in the lattice thermal conductivity. © *1998 American Institute of Physics.* [S0021-8979(98)03023-0]

I. INTRODUCTION

The search for superior thermoelectric materials generally requires finding conditions such that the thermoelectric figure of merit

$$\mathrm{ZT}=\frac{S^2\sigma T}{\kappa_{\mathrm{ph}}+\kappa_e} \tag{1}$$

is as large as possible. Here, S is the Seebeck coefficient, σ is the electrical conductivity, κ_{ph} is the lattice (phonon) thermal conductivity, κ_e is the electronic thermal conductivity, and T is the absolute temperature. Most of the methods to improve ZT were formulated as early as the 1960s, and usually could be reduced to the requirement to limit the phonon propagation while not significantly deteriorating electron transport through the sample.[1]

A rebirth of the field of thermoelectrics[2] was brought forward by the emergence of large numbers of new artificially synthesized materials, including different types of semiconductor low-dimensional structures. Low-dimensional confinement allows for more degrees of freedom for maximizing ZT. The experimentally observed increase of the Seebeck coefficient in $PbTe/Pb_{1-x}Eu_xTe$ and SiGe/Si multiple-quantum well structures gives apparent confirmation of the usefulness of low dimensionality.[3]

Theoretical predictions[4,5] of a strong enhancement of the figure of merit for semiconductor superlattices and quantum wells were based on the modification of k_e and $S^2\sigma$ product due to the spatial confinement of carriers and the corresponding change in the carrier density of states. Meanwhile these predictions ignored the effects of spatial confinement of phonons, and used bulk values of κ_l. This approximation is valid for quantum well structures with boundaries made out of a material with similar crystalline and elastic properties where phonon modes extend through the boundaries and do not differ significantly from the bulk. However, it should be pointed out that even in superlattices of similar materials, the phonon transport can be modified due to miniband formation and the emergence of mini-Umklapp processes.[6]

The situation is significantly different in the quantum wells, which are either free standing or embedded within the rigid material with distinctively different elastic properties. Here, phonon dispersion and group velocities are changed due to the spatial confinement induced by the boundaries. The phonon confinement affects all phonon relaxation rates, and makes the thermal transport properties of nanostructures rather different from those of bulk material. These conditions are characteristic of many realistic experiments with thermoelectrics.

In this paper, we study how spatial confinement of acoustic phonon modes changes the thermoelectric figure of merit of quantum well structures via modification of the lateral lattice thermal conductivity. The paper is organized as follows. In Sec. II we present the theory. Results of the numerical simulations and discussion are given in Sec. III. We present our conclusions in Sec. IV.

II. THEORY

A. Thermoelectric figure of merit

As an illustrative example, we will consider a bismuth–telluride quantum well structure. We have chosen this material because it has bulk superior thermoelectric properties. The model presented will, of cause, be applicable for other material systems. In order to have a pronounced phonon confinement effect, the quantum well structure (thin film) should be embedded within material with distinctively different elastic (crystalline) properties. One of the possibilities is a Bi_2Te_3 film on polyimide or mica as described in Ref. 7. In the case of polyimide, the quantum well boundaries can be considered as free surface since they are surrounded by the air and soft polymer. Multiple quantum well structures can also be made this way by sandwitching bismuth–telluride thin films between layers of polymer or other ''soft'' dielectric.[7,8] The well width W in such structures should be

[a]Electronic mail: alexb@ee.ucla.edu

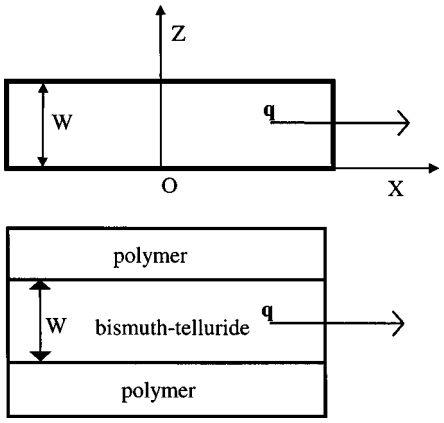

FIG. 1. Geometry of the quantum well structure with free-surface boundaries used for model simulations (upper). Geometry of the corresponding experimental structure (lower).

rather small (less than 50 nm) for strong phonon confinement effects. The geometry of the structure and notations are shown in Fig. 1.

Our model will use the derivations of thermoelectric parameters for two-dimensional (2D) structures given in Ref. 4. However, we do not assume that $k_{\rm ph}$ equals to its bulk value $k_{\rm ph}^{\rm bulk}$. Rather, we calculate $k_{\rm ph}$ as a function of the well width W and temperature T. A significant dependence of $k_{\rm ph}$ on W is expected from the spatial confinement of phonons participating in thermal transport, mainly through the change of their group velocity. Since we are interested in operation at the room and above temperatures, no phonon drag effect will be considered. We also assume that the confinement of phonon modes does not strongly affect electron–phonon scattering rates. The latter was recently shown in Ref. 9.

For conduction along the x axis, one can write in the one-band material approximation

$$S=-\frac{k_B}{e}(2F_1/F_0-\chi_{\rm 2D}^*), \tag{2}$$

$$\sigma=\frac{1}{2\pi W}\left(\frac{2k_BT}{\hbar^2}\right)(m_xm_y)^{1/2}F_0e\mu_x, \tag{3}$$

$$k_e=\frac{\langle\tau\rangle\hbar^2}{4\pi W}\left(\frac{2k_BT}{\hbar^2}\right)^2(m_y/m_x)^{1/2}k_B(3F_2-4F_1^2/F_0), \tag{4}$$

$$\kappa_{\rm ph}=\frac{k_B}{2\pi^2v}\left(\frac{k_B}{\hbar}\right)^3T^3\int_0^{\theta/T}\frac{\tau_C\xi^4e^\xi}{(e^\xi-1)^2}d\xi. \tag{5}$$

Here k_B is the Boltzmann constant, $\hbar$ is the Plank constant, e is the electron charge, $m_{x,y,z}$ are three components of the effective-mass tensor, μ_x is the mobility along the x axis, $\langle\tau\rangle(=\mu_xm_x/e)$ is the electron relaxation time which is assumed to be constant as in Ref. 4, θ is the Debye temperature, $\hbar\omega$ is the phonon energy, $\xi=\hbar\omega/k_BT$, $\tau_C\equiv\tau(W,T)$ is the combined phonon relaxation time due to all resistive processes, v is the velocity of sound, $\chi_{\rm 2D}^*$ is the reduced chemical potential for quasi two-dimensional structures, and F_p are the Fermi–Dirac functions. The reduced chemical potential is defined (by analogy with the electochemical potential) as

$$\chi_{\rm 2D}^*\equiv\frac{\chi^{\rm 2D}}{k_BT}=\frac{1}{k_BT}\left(\chi^{\rm 3D}-\frac{\hbar^2\pi^2}{2m_zW^2}\right), \tag{6}$$

where three-dimensional chemical potential $\chi^{\rm 3D}$ is determined by the doping and related to the Fermi energy E_F and density of states $N(E)$ as

$$\chi^{\rm 3D}=E_F-\frac{\pi^2k_B^2T^2}{6}\frac{d}{dE}[\ln N(E)]$$

$$\approx E_F-\frac{\pi^2k_B^2T^2}{12E_F}. \tag{7}$$

Equations (2)–(4) are valid for anisotropic material with a parabolic band and are not restricted to semiconductors alone.

B. Lattice thermal conductivity

To calculate the lattice thermal conductivity in Eq. (5), we need to determine the scattering rate τ_C^{-1} as a function of the well width and temperature. It is well known that only those processes which do not conserve crystal momentum contribute to the lattice thermal resistance.[10] These processes, referred to as resistive, are boundary scattering, mass-difference scattering, scattering on dislocations, and three-phonon Umklapp scattering processes. Equation (5) which we added to the thermoelectrics 2D formalism of Eqs. (2)–(4) is written under the assumption that such resistive processes are dominant over the normal phonon processes.

Limiting our consideration to the above mentioned resistive processes, we proceed with the Matthiessen's rule

$$\frac{1}{\tau_C}=\frac{1}{\tau_U}+\frac{1}{\tau_I}+\frac{1}{\tau_D}+\frac{1}{\tau_B}, \tag{8}$$

where τ_U, τ_I, τ_D, and τ_B are the relaxation times due to the U-processes through all allowed channels: the mass-difference (or isotop) scattering, scattering on dislocations, and boundary scattering, respectively. In order to evaluate relaxation rates of Eq. (8), we should use the actual dispersion relations (for the Umklapp processes) and group velocities $v_g\equiv v_g[\omega(q)]$ for phonons in a quantum well (q is the phonon in-plane wave vector). Modification of the wave vector selection and frequency conservation rules due to the spatial confinement should also be taken into account.

The phonon relaxation mechanism which is strongly affected by the change in the average phonon group velocity is the mass-difference scattering. The phonon relaxation rate due to interaction with atoms of different masses is given by[10]

$$\frac{1}{\tau_I}=\frac{V_0\omega^4}{4\pi v_g^3}\sum_i f_i[1-(M_i/M)]^2, \tag{9}$$

where V_0 is the volume per atom, M_i is the mass of an atom, and f_i is the fractional content of atoms with mass M_i which is different from M. Writing Eq. (9) we tacitly neglected additional terms associated with the difference of stiffness constants of the nearest-neighbor bonds. The phonon scattering on dislocations can be evaluated using the relation[10]

$$\frac{1}{\tau_D} = \frac{N_d a^4 \omega^3}{v_g^2}, \tag{10}$$

where N_d is the number of dislocation lines per unit area, and a is the lattice constant.

The expression for τ_U of a thermal mode with the wave vector q in the single-mode relaxation rate approximation can be found in Ref. 11. A detailed study of the effects of phonon confinement on three-phonon Umklapp processes and, correspondingly, on τ_U was reported elsewhere.[12]

Boundaries of nanostructures also contribute to phonon scattering. Since boundary scattering is almost independent of frequency and its relevant contribution becomes significant at low temperatures (not considered in this paper), we limit our consideration to a simple estimate of the phonon relaxation rate from the semiempirical relation

$$\frac{1}{\tau_B} = \frac{v_g}{W}. \tag{11}$$

The phonon relaxation due to scattering from the grain boundaries is not included in our model. This mechanism is irrelevant for crystalline bismuth telluride and for the polycrystalline material, in which the grain size is usually bigger than the phonon mean free path and W considered here.

C. Confinement of acoustic phonons

In order to evaluate the relaxation rates in Eqs. (8)–(11), we have to determine the dependencies of $v_g(q)$ and $\omega(q)$ on the well width W. The dispersion of the confined phonon modes can be found in the continuous medium approximation by solving the elasticity equation with given boundary conditions (free-surface boundaries). In order to do it, we follow prescriptions of Refs. 13 and 14. Since here we are mostly interested in the value of the average phonon group velocities, we will briefly outline the procedure and present the results.

The normal components of the stress tensor on the free-surface boundaries must vanish. These boundary conditions bring about a significant change to the phonon dispersion and group velocities as compared to bulk. One should note here that a significant modification of phonon modes can be attained not only in a free-surface nanostructure but also in a nanostructure embedded within rigid material. In this case, the normal components of the stress tensor are unrestricted but the displacement is zero at the boundary. This corresponds to the clamped-surface boundary conditions.[15] As we mentioned in the beginning of Sec. II, our choice of the material system corresponds to the free-surface boundary conditions.

Solving numerically the elasticity equation, we first find confined phonon modes $\omega_n^t(q)$ for a particular well width and material parameters and then, by numerical differentiation, determine the group velocities. Subscript t defines the type of the phonon modes which are characterized by their distinctive symmetries (shear, dilatational, and flexural modes). The phonon group velocity for each mode type in the nth branch is defined as $v_g^{t,n} = \partial \omega_n^t / \partial q$.

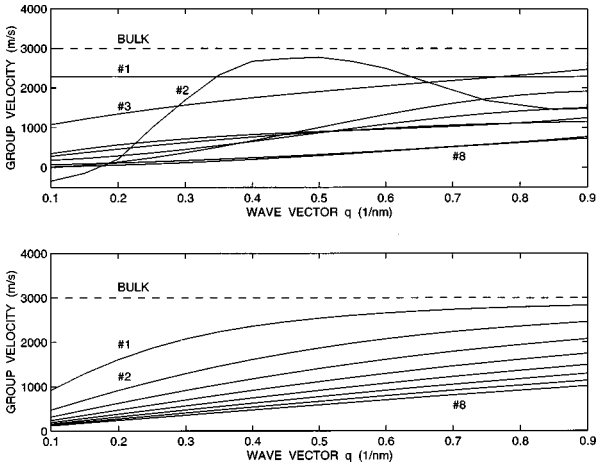

FIG. 2. Group velocity as a function of in-plane wave vector for the dilatational (upper) and shear (lower) modes in a 100 Å wide bismuth–telluride quantum well. The result are shown for eight lowest phonon modes. The dashed lines show the average group velocity for bulk material. It is easy to see that the phonon group velocities are lower than in bulk, and decrease with increasing mode number.

III. NUMERICAL RESULTS

A. Lattice thermal conductivity

The phonon group velocities as functions of the phonon wave vector q along the propagation direction are presented in Fig. 2. The typical results are shown for the lowest dilatational (upper part) and shear (lower part) type modes ($n = 1, \cdots, 8$) in a 100 Å wide quantum well. Due to spatial confinement, many more branches of each polarizational type are present in the quantum well as compared to the bulk. One can easily see the general trend: the higher the mode number the smaller the group velocity over the range of wave vector values. The group velocity of thermal modes decreases to as much as 3–4 times ($n \approx 40$ for $W = 100$ Å at room temperature). For comparison the average sound velocity of the bulk is shown by dashed lines. The change of polarization types and the $\omega \equiv \omega(q)$ dependence due to confinement brings also modifications of the energy and momentum conservation laws. The latter is important for calculation of the lattice thermal conductivity of quantum wells and was discussed by us in Ref. 12.

Once the phonon dispersion and group velocities are calculated, we evaluate phonon scattering rates and lattice thermal conductivity for a bulk Bi_2Te_3 slab and quantum wells over the range of temperatures and well widths. The material parameters used in simulation are summarized in Table I (the

TABLE I. Material parameters for Bi_2Te_3 used for simulation.

$a = 4.3835$ Å
$a' = 30.360$ Å
$m_x = 0.012 m_0$
$m_y = 0.081 m_0$
$m_z = 0.32 m_0$
$v = 3 \times 10^3$ m/s
$\mu_x = 1500$ cm^2/V s
$M(\mathrm{Bi}) = 3.47 \times 10^{-25}$ kg
$M(\mathrm{Te}) = 2.12 \times 10^{-25}$ kg

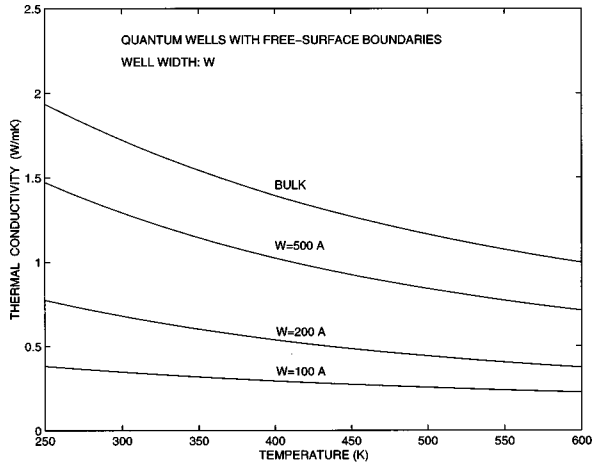

FIG. 3. Lattice thermal conductivity of bismuth–telluride as a function of temperature for bulk material and three different quantum wells. The calculations are performed for quantum wells with free-surface boundaries. Significant drop of thermal conductivity is due to spatial confinement of acoustic phonons.

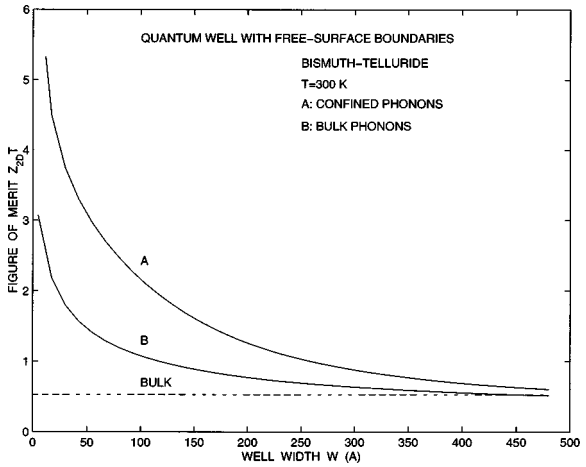

FIG. 4. Thermoelectric figure of merit ZT of bismuth–telluride as a function of quantum well width. The results are shown for quantum wells with confined (denoted by A) and bulk phonons (denoted by B). The figure of merit for bulk bismuth–telluride calculated with the same material parameters is also shown. Additional increase of ZT arises from the decrease of the lattice thermal conductivity due to phonon confinement.

values are after Refs. 16 and 17). The overall phonon scattering rate increases in a quantum well. A significant drop in the average phonon group velocity (see Fig. 2) strongly increases phonon relaxation rates via mass-difference scattering and scattering on dislocations as expected from Eqs. (9) and (10). The three-phonon Umklapp scattering is also becoming more effective. Boundary scattering (or grain boundary scattering) is less sensitive to the phonon group velocity change and just slightly offsets the final result. One important thing to note is that by improving crystal and surface quality one can reduce the impurity and boundary scattering rates but not the Umklapp scattering rate. The increase of the Umklapp process scattering rate in a quantum well is a direct result of the modification of phonon dispersion due to spatial confinement of the phonon modes. In Fig. 3 we show the lattice thermal conductivity $k_{\mathrm{ph}}(W,T)$ as a function of the temperature for different quantum well widths and the bulk material. One can see that k_{ph} for a 100 Å wide well is much smaller than that of a bulk, particularly at room and slightly below room temperatures.

In order to verify the accuracy of our model for k_{ph}, we apply it to different material systems and compare the results with available experimental data. We found that our numerical results are consistent with experimental data presented in Ref. 7. It was reported there that the lattice thermal conductivity of the Bi_2Te_3 films (0.5–3 μm thick) is considerably lower than k_{ph} of bulk crystals of the same solid solution. At room temperature, $k_{\mathrm{ph}} \approx 1.2$ W/m K was measured as compared to the bulk value of 1.7 W/m K. It is reasonable to expect that further decrease of the film thickness will bring about an additional decrease in the thermal conductivity. Experimentally observed temperature dependence in Ref. 7 is very close to that calculated on the basis of our model.

B. Thermoelectric figure of merit

After determining $k_{\mathrm{ph}} = k(W,T)$, we can calculate ZT using Eqs. (1)–(5). Material parameters used for simulation are the same as in Table I. To obtain high ZT, we optimize $\chi^*_{2\mathrm{D}}$ by choosing an appropriate carrier concentration (doping level) for a particular well width. The optimum $\chi^*_{2\mathrm{D}}$ occurs when we start with $\chi_{3\mathrm{D}}$ slightly above the conduction band which corresponds to a partially degenerate *n*-type semiconductor. We also determine that $\chi^*_{2\mathrm{D}}$ lies below the second confined electron state (one-band model). The Fermi–Dirac functions are calculated using the known expansions[18] for integer *p*.

The thermoelectric figure of merit ZT as a function of quantum well width is shown in Fig. 4 with and without phonon confinement effects. The calculations were performed for room temperature. As one can see from Fig. 4, the decrease of k_{ph} due to the spatial confinement of phonons in a quantum well embedded within a material of different elastic properties leads to a noticeable increase of ZT as compared to the case without the phonon confinement. This additional increase is particularly significant for the intermediate and thin quantum wells with $W \approx 90-300$ Å. The general trend of increasing ZT with the reduction of the well width is characteristic for both cases. The latter is expected due to the increased carrier confinement in narrower wells and basically is the result of the effectively 2D density of states for free carriers.[3–5] The additional increase of ZT due to the confinement of phonons can be as large as two times the value without the phonon confinement for a 90 Å wide quantum well with free-surface boundary conditions (room temperature). This additional increase is clearly seen in Fig. 4.

Although our model assumed a quantum well with free-surface boundary conditions, the conclusions about increased ZT due to the phonon confinement can be extended to quantum wells with clamped-surface boundary conditions (rigid boundaries). The lowest confined phonon modes in quantum wells embedded within rigid materials are higher in energy than those in a free-standing quantum well, but the overall behavior and the decrease of the group velocities are very similar in both cases. The model presented here can be de-

veloped further to include mixed boundary conditions and the interface quality.

The most vulnerable approximation used in our model as well as in models of Refs. 4 and 5 is the assumption of a constant electron relaxation rate. This led to the use of the constant carrier mobility which was equal to that of the bulk material. Our estimations show that the error due to this assumption may significantly offset the value of ZT for $W \leqslant 15-20$ Å, although for wider wells, the treatment is acceptable. A rigorous self-consistent theory would require the solution of the Boltzmann equation with the scattering probabilities determined for confined electron–confined phonon interaction. Such work is currently in progress.[19]

IV. CONCLUSIONS

We have studied the effects of phonon spatial confinement on the thermoelectric figure of merit for quantum well structures. As a prototype structure for illustrating the effect, we have used a free-standing bismuth–telluride thin film, although our model can be extended to other quantum well structures embedded within material with distinctly different elastic properties. It was shown that strong modification of the phonon group velocities and dispersion due to spatial confinement leads to a significant increase of the phonon relaxation rates and, as a result, a strong drop in the lattice thermal conductivity k_{ph}. From the numerical calculations, we predicted that due to the decrease of k_{ph}, the thermoelectric figure of merit experiences an additional increase (factor of 2 for 90 Å wide well at 300 K) as compared to the structures with bulk phonons. The active (not via temperature) phonon engineering discussed in this paper may eventually lead to the improvement of thermoelectric properties of the nanostructured materials.

ACKNOWLEDGMENTS

The authors are indebted to Professor M.S. Dresselhaus (MIT) and Professor G. Chen (UCLA) for discussions on low-dimensional thermoelectrics. This work was supported by the DoD MURI-ONR program on Thermoelectrics (Dr. John Pazik) and DoD MURI-ARO program on Low Power Electronics (Dr. James Harvey).

[1] A. F. Ioffe, *Semiconductor Thermoelements and Thermoelectronic Cooling* (Infosearch, London, 1957); A. F. Ioffe, *Semiconductor Thermoelements* (Nauka, Moscow, 1956) (in Russian).
[2] G. Mahan, B. Sales, and J. Sharp, Phys. Today **50**, 42 (1997).
[3] L. D. Hicks, T. C. Harman, X. Sun, and M. S. Dresselhaus, Phys. Rev. B **53**, R10493 (1996); T. C. Harman, D. L. Spears, D. R. Calawa, S. H. Groves, and M. P. Walsh, in Proceedings of the 16th International Conference on Thermoelectrics, ICT'97, Dresden, Germany IEEE, 1997, IEEE Cat. No. 97TH8291, p. 416; A. Yamamoto, H. Kato, S. Kuwashiro, M. Takimoto, T. Ohta, K. Miki, K. Sakamoto, T. Matsui, and K. Kamisako, *ibid.*, p. 434.
[4] L. D. Hicks and M. S. Dresselhaus, Phys. Rev. B **47**, 12727 (1993); L. D. Hicks, T. C. Harman, and M. S. Dresselhaus, Appl. Phys. Lett. **63**, 3230 (1993).
[5] J. O. Sofo and G. D. Mahan, Appl. Phys. Lett. **65**, 2690 (1994); G. D. Mahan and H. B. Lyon, Jr., J. Appl. Phys. **76**, 1899 (1994); D. A. Broido and T. L. Reinecke, Phys. Rev. B **51**, 13797 (1995).
[6] S. Y. Ren and J. D. Dow, Phys. Rev. B **25**, 3750 (1982).
[7] Yu. Boikov, B. M. Goltsman, and V. A. Danilov, Semiconductors **29**, 464 (1995).
[8] K. L. Wang and A. Balandin (unpublished).
[9] N. Nishiguchi, Phys. Rev. B **54**, 1494 (1996).
[10] P. G. Klemens, in *Solid State Physics*, edited by F. Seitz and D. Turnbull (Academic, New York, 1958), Vol. 7, p. 1; J. E. Parrott and A. D. Stuckes *Thermal Conductivity of Solids* (Methuen, New York, 1975).
[11] Y.-J. Han and P. G. Klemens, Phys. Rev. B **48**, 6033 (1993).
[12] A. Balandin and K. L. Wang, Phys. Rev. B **58**, 1544 (1998).
[13] SeGi Yu, K. W. Kim, M. A. Stroscio, G. J. Iafrate, and A. Ballato, Phys. Rev. B **50**, 1733 (1994); N. Bannov, V. Aristov, and V. Mitin, *ibid.* **51**, 9930 (1995).
[14] A. Svizhenko, A. Balandin, S. Bandyopadhyay, and M. A. Stroscio, Phys. Rev. B **57**, 4687 (1998).
[15] P. M. Morse, *Vibration and Sound* (American Institute of Physics, New York, 1986).
[16] H. Scherrer and S. Scherrer in *CRC Handbook of Thermoelectrics*, edited by D. M. Rowe (Chemical Rubber Corporation, Boca Raton, FL, 1995), p. 211.
[17] R. D. Barnard, *Thermoelectricity in Metals and Alloys* (Taylor & Francis Ltd., London, 1972); T. C. Harman and J. M. Honig, *Thermoelectric and Thermomagnetic Effects and Applications* (McGraw–Hill, New York, 1967).
[18] R. B. Dingle, Appl. Sci. Res., Sect. B **6**, 225 (1957).
[19] A. Balandin and K. L. Wang, Bull. Am. Phys. Soc. **43**, 80 (1998).